Co-based ternary bulk metallic glasses with ultrahigh strength and plasticity

Jianfeng Wang, Ran Li,[a] Nengbin Hua, and Tao Zhang[b]
Key Laboratory of Aerospace Materials and Performance (Ministry of Education), School of Material Science and Engineering, Beihang University, Beijing 100191, People's Republic of China

(Received 16 January 2011; accepted 3 May 2011)

A family of ultrahigh strength Co-based bulk metallic glasses (BMGs) with critical diameters up to 2 mm is synthesized in $Co_{65-x}Ta_xB_{35}$ (at.%, x = 5–10) alloys by copper mold casting. The improved glass-forming ability associated with near eutectic compositions is attributed to the appropriate addition of Ta. The glassy alloys exhibit high glass transition temperature of 930–975 K, ultrahigh compressive strength of 5.6–6.0 GPa, high specific strength of 639–654 N·m/g, Vickers hardness of 15–16 GPa, and distinct plastic strain of 0.5–1.5%. The strength and the specific strength are the highest values reported for bulk metallic materials known so far. Several universal criteria correlated with the thermal properties, elastic constants, and mechanical properties were validated in the Co-based BMG system. These Co–Ta–B BMGs combining with superior mechanical properties, high thermal stability, and simple elemental composition are significant for scientific research as modeling materials and industrial application as advanced structural materials.

I. INTRODUCTION

Compared with crystalline alloy materials, bulk metallic glasses (BMGs) exhibit higher strength and specific strength due to their disordered structures and structural uniformity.[1–3] Intensive efforts including the optimization of alloy composition, enhancement of glass-forming ability (GFA), and improvement of mechanical properties have been made due to their great potential application as advanced structural materials.[3–5] How to design desirable BMGs with superhigh mechanical strength has brought up extensive attention. It has been clarified that there exists universal linear relationships between strength and Young's modulus (E) or shear modulus (G) for metallic glasses.[6–8] Generally, elastic constants (M) of a designed glassy alloy are related to those of the constituent elements. It can be roughly calculated with an equation of $M^{-1}=\sum f_i M_i^{-1}$, where M_i and f_i denote the corresponding elastic constant and atomic concentration of the constituent elements, respectively.[9,10] On the other hand, metallic glasses containing small-atomic size metalloid exhibit higher elastic moduli due to the formation of local solute-centered coordination polyhedra, which are the manifestation of intensive chemical short-range order caused by the strong covalent metal–metalloid bonds.[11] Moreover, the elastic moduli and mechanical properties of metallic glasses can be improved by appropriately tuning the fraction of metalloid elements.[12] Therefore, it is advantageous to design a high-strength metallic glass consisting of metallic elements with high elastic moduli and metalloid elements with appropriate chemical interaction.

Co-based BMG alloys with high GFA are among the best candidates to develop new structural metallic materials with ultrahigh strengths and elastic moduli. For example, Co–Fe–Si–B–Nb BMGs with high E of about 210 GPa show high strengths exceeding 4000 MPa.[13] Co–Fe–Ta–B glassy alloy, which is the strongest bulk metallic material known so far, exhibits ultrahigh fracture strength and high E reaching 5185 MPa and 268 GPa, respectively.[14] These results shed light on the design of metallic glasses with ultrahigh strength.

In this article, B-rich $Co_{65}B_{35}$ binary alloy is selected as a precursor alloy according to the above analysis. GFA of this Co–B binary alloy is not high enough to produce bulk samples (J.F. Wang and T. Zhang, unpublished data). Ta element is selected to partially substitute for Co based on the large mismatch in atomic sizes and moderate negative heating of mixing for Ta–Co and Ta–B atomic pairs, which are beneficial for the improvement of GFA,[15,16] together with the high elastic moduli of Ta compared with most of other metallic elements.[17] Glass formation and thermal and mechanical properties of the designed $Co_{65-x}Ta_xB_{35}$ (at.%, x = 5–10) alloys were evaluated. These alloys exhibit high GFA, ultrahigh strength and specific strength, high Vickers hardness, and distinct plastic deformation. The relationships between the excellent compressive mechanical properties and other physical properties related to the elastic moduli and thermal properties for the alloys are discussed.

Address all correspondence to these authors.
[a]e-mail: liran@buaa.edu.cn
[b]e-mail: zhangtao@buaa.edu.cn
DOI: 10.1557/jmr.2011.187

 © Materials Research Society 2011

https://doi.org/10.1557/jmr.2011.187 Published online by Cambridge University Press

II. EXPERIMENTAL

A Co–B prealloy with B content of 40 at.% was prepared by induction melting pure Co (99.9 mass%) and pure B (99.99 mass%) in a high-purity argon atmosphere. Co-based alloys with a nominal composition of $Co_{65-x}Ta_xB_{35}$ (at.%, x = 5–10) were then prepared by arc melting the mixings of pure Co, Ta (99.99 mass%) metal, and the Co–B prealloy in a Ti-gettered high-purity argon atmosphere. The ingots were remelted several times to ensure homogeneity. BMGs with diameters up to 2 mm were produced by injection mold casting method. Ribbons of these alloys with a dimension of ~50 μm in thickness and ~2 mm in width were prepared by the single-roller melt-spinning method.

The amorphous structure of the as-cast and as-spun samples was identified by x-ray diffraction (XRD) using a Dmax2200PC Rigaku x-ray diffractometer with Cu $K\alpha$ radiation (Rigaku, Tokyo, Japan). The thermal properties characterized by glass transition, crystallization, and melting behaviors were investigated by a NETZSCH DSC 404 C differential scanning calorimetry (DSC; NETZSCH, Selb, Germany) at a heating rate of 0.67 K/s for low-temperature region and a relatively low heating rate of 0.33 K/s for high-temperature region. Uniaxial compression testing was conducted at an ambient temperature using mechanical testing machine at a strain rate of 4.2×10^{-4} s^{-1}. The testing samples with a gauge aspect ratio of 2:1 were cut from the as-cast 1-mm cylindrical rods. The compression tests were performed at least in triplicate for each BMG. Deformation and fracture morphologies were observed with JSM 5800 scanning electron microscopy (SEM, Tokyo, Japan). Vickers hardness (H_v) was measured using a Vickers hardness indenter with a load of 1.96 N and a loading time of 10 s. At least seven indents were performed for each sample and the average value was adopted. The density (ρ) was measured by Archimedes' method using a Sartorius balance (Readability: 10 μg) (Sartorius, Gottingen, Germany). The elastic properties were determined with an Olympus Panametrics-NDT 5900PR ultrasonic testing device (Olympus, Waltham, MA) using ultrasonic pulse-echo techniques. Glassy samples with a dimension of 2 mm in diameter and 4 mm in length were adopted for these measurements. The elastic constants, i.e., Poisson's ratio (ν), Young's modulus (E), shear modulus (G), and bulk modulus (B), can be calculated using the measured data of longitudinal and transverse sound velocities (v_l and v_t). The error bands of the calculation elastic constants are below 5%.

III. RESULTS AND DISCUSSION

A. Glass formation and thermal properties

Figure 1 shows the XRD patterns of the as-cast glassy rods of $Co_{65-x}Ta_xB_{35}$ (at.%, x = 5–10) alloys with maximal diameters. Only a broad diffuse peak is observed

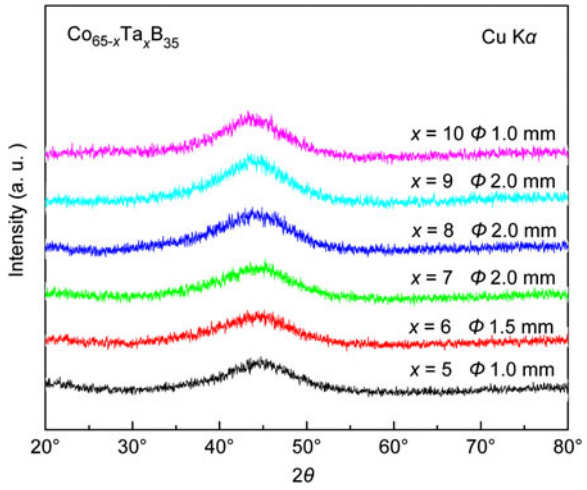


FIG. 1. X-ray diffraction patterns of $Co_{65-x}Ta_xB_{35}$ (at.%, x = 5–10) bulk metallic glasses (BMGs).

for each pattern, indicating the fully amorphous structure of these samples within the resolution of the x-ray measurement conditions. For comparison, the GFA of binary $Co_{65}B_{35}$ alloy (J.F. Wang and T. Zhang, unpublished data) without Ta was also evaluated, as listed in Table I. The critical size for glass formation (d_c) can be significantly increased from ~0.05 mm in thickness for binary $Co_{65}B_{35}$ alloy to 2 mm in diameter for ternary $Co_{65-x}Ta_xB_{35}$ with x = 7–9. The introduction of Ta with proper contents is beneficial to the improvement of GFA of the resulting alloys.

The glass transition, crystallization, and melting behavior of these glassy alloys are shown in Figs. 2(a) and 2(b). Characteristic temperatures, i.e., the glass transition temperature (T_g), the onset temperature of crystallization (T_x), the melting temperature (T_m), and the liquidus temperature (T_l) of the Co-based BMGs are listed in Table I. Distinct glass transition followed by a wide supercooled liquid region before crystallization can be observed in Fig. 2(a). With the increase of Ta content from 5 to 10 at.%, T_g increases from 930 to 975 K and the supercooled liquid region ΔT_x ($\Delta T_x = T_x - T_g$) coincidently enlarges from 41 to 68 K, which indicate that the thermal stability can be improved by the introduction of Ta. Different from T_g and ΔT_x, T_l first decreases with increasing Ta content, reaching a minimum value of 1492 K at 8 at.% Ta, and followed by a remarkable increase with the further increase of Ta content. The T_m remains almost unchanged over the whole content range of Ta substitutions. The melting behavior for the alloys with 5 at.%Ta takes place through two endothermic stages. The temperature interval between two endothermic peaks gradually decreases with increasing Ta content until two peaks merge into a single endothermic peak at 8 at.%Ta. Further increase of Ta content to 10 at.% induces a deviation from the eutectic

https://doi.org/10.1557/jmr.2011.187 Published online by Cambridge University Press

TABLE I. The critical sizes (d_c), thermal properties, and parameters of $Co_{65-x}Ta_xB_{35}$ (at.%, x = 0, 5–10) glassy alloys. T_g, T_x, T_m, and T_l are the glass transition temperature, the onset temperature of crystallization, the melting temperature, and the liquidus temperatures, respectively. $\Delta T_x = T_x - T_g$, $T_{rg} = T_g/T_l$, $\gamma = T_x/(T_g + T_l)$, and α is a parameter described in Ref. 18.

Alloys	d_c (mm)	T_g (K)	T_x (K)	T_m (K)	T_l (K)	ΔT_x (K)	T_{rg}	γ	α
$Co_{65}B_{35}$	~0.05	–	740	1507	1582	–	0.47	–	1.08
$Co_{60}Ta_5B_{35}$	1.0	930	971	1461	1523	41	0.61	0.395	1.17
$Co_{59}Ta_6B_{35}$	1.5	934	981	1461	1513	47	0.62	0.401	1.18
$Co_{58}Ta_7B_{35}$	2.0	945	996	1460	1510	51	0.63	0.406	1.20
$Co_{57}Ta_8B_{35}$	2.0	951	1005	1458	1492	54	0.64	0.411	1.23
$Co_{56}Ta_9B_{35}$	2.0	961	1020	1460	1527	59	0.63	0.409	1.21
$Co_{55}Ta_{10}B_{35}$	1.0	975	1043	1462	1542	68	0.63	0.414	1.20

point. All these melting behaviors indicate that the present alloys exhibit the same eutectic event, and the alloy with 8 at.%Ta is the closest to the eutectic point. The Co–Ta–B alloys with the Ta content of 7–9 at.% with the highest GFA lie in the vicinity of eutectic point according to the XRD and DSC analyses. This result is consistent with the well-known principle that deep eutectic is preferable for glass formation.[19–21]

A lot of glass-forming criteria related with thermal properties, e.g., the reduced glass transition temperature ($T_{rg} = T_g/T_l$) proposed by Turnbull,[22] the supercooled liquid region ($\Delta T_x = T_x - T_g$) by Inoue et al.,[23] γ parameter [$\gamma = T_x/(T_g + T_l)$] by Lu and Liu,[24] and α parameter ($a = \frac{\sum_{i=1}^{n} c_i T_i}{T_l}$, where c_i and T_i are the atomic fraction and melting temperature of element i, respectively, and T_l is the liquidus temperture of alloy) by Davies and Lewis,[18] have been extensively used to predict and elucidate GFA of various kinds of metallic glasses. These glass-forming parameters of the Co–Ta–B BMGs are listed in Table I. For comparison, the data of $Co_{65}B_{35}$ alloy are also listed (J.F. Wang and T. Zhang, unpublished data).Compared with the $Co_{65}B_{35}$ binary alloy, the $Co_{65-x}Ta_xB_{35}$ (at.%, x = 5–10) alloys exhibit higher T_{rg} of 0.61–0.64, wider ΔT_x of 41–68 K, larger γ parameters of 0.395–0.414, and larger α of 1.17–1.23 due to the addition of Ta element. Thus, the introduction of Ta in Co–B alloy is beneficial to stabilize supercooled liquid and promote GFA. However, it can be noticed that quantitative correlation between all of the glass-forming parameters and the experimentally determined GFA reflected by d_c is not strictly followed as listed in Table I. Only the tendency for the change of T_{rg} and α, strongly determined by the appearance of eutectic point at 8 at.%Ta, is approximately consistent with the variation of d_c. These disagreements have also been reported for other BMG systems.[25–28] Therefore, the glass-forming criteria can be only assistant in optimizing the composition for high GFA but cannot be considered as accurate indicators for the composition prediction.

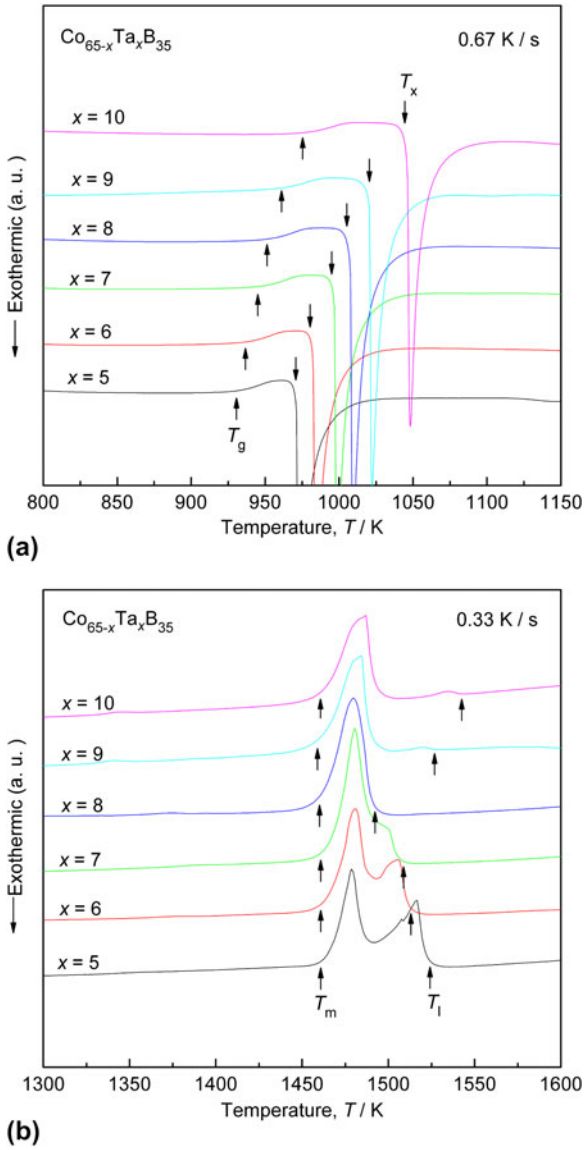


FIG. 2. Differential scanning calorimetry curves of $Co_{65-x}Ta_xB_{35}$ (at.%, x = 5–10) BMGs: (a) glass transition and crystallization behaviors at a heating rate of 0.67 K/s; (b) melting behaviors at a heating rate of 0.33 K/s.

B. Mechanical properties of Co–Ta–B BMGs

Figure 3 shows the true compressive strain–stress curves for the $Co_{65-x}Ta_xB_{35}$ ternary alloy rods. With the increment of Ta content, the yield strength (σ_y) and compressive strength (σ_c) increase gradually, whereas the plastic strain (ε_p) is depressed. The Co–Ta–B BMGs exhibit ultrahigh σ_y of 5.2–5.6 GPa and σ_c of 5.6–6.0 GPa, as well as distinct ε_p of 0.5–1.5%. The specific strength of the Co–Ta–B BMGs is also calculated as 639–654 N·m/g, which is as high as widely used carbon-fiber-reinforced polymers in aerospace and automotive fields, but whose strength is 6 times lower.[29] The strength and specific strength are higher than those of any bulk

https://doi.org/10.1557/jmr.2011.187 Published online by Cambridge University Press

crystalline or glassy alloys so far reported.[3,29] The Co-based BMGs also present high Vickers hardness (H_v) up to 16.1 GPa, which is slightly lower than $W_{46}Ru_{37}B_{17}$ alloy, the hardest amorphous alloy known so far.[30] However, bulk samples of the W–Ru–B alloy cannot be produced because of its poor GFA.

As a typical sample, the deformed and fracture specimens of $Co_{60}Ta_5B_{35}$ BMG were investigated by SEM. Figure 4(a) displays the lateral morphology of the cylindrical sample unloaded after ~1.2% plastic deformation. Multishear bands and shear steps are visible on the sample face responsible for the significant plastic deformation. The multishear bands are composed of two kinds: the primary shear bands that are declined by ~45 degree to the direction of applied load and the secondary shear bands developed by branching and interaction of the primary ones and tilted at ~45 degree to the main shear planes. A crack, as shown in Fig. 4(a), formed from the top surface and propagated along axial direction, is associated with the fracture failure of whole sample. After fracture, the sample splits into pieces of small fragments as shown in Fig. 4(b), similar to other brittle Fe- and Co-based BMGs.[13,31–34] The fracture surface of the fragments exhibits mixed feature composed of shell-like and vein-like patterns, which are characteristics of fracture surface for brittle and plastic metallic glasses, as shown in Figs. 4(c) and 4(d). Microcracks are visible in the fragments with both kinds of patterns identified by arrows. It is suggested that the rapid propagation of microcracks associated with instability of multishear bands is responsible for the fragmented fracture.

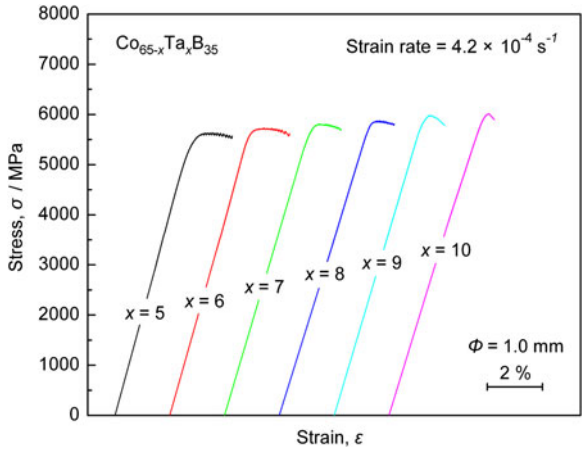


FIG. 3. Compressive true stress–strain curves of $Co_{65-x}Ta_xB_{35}$ (at.%, x = 5–10) glassy rods.

Recently, a possible correlation of plasticity and elastic properties, related to G/B (where G is shear modulus, B is bulk modulus) and v (where v is Poisson's ratio), for BMGs was reported.[9,10,35] It is claimed that metallic

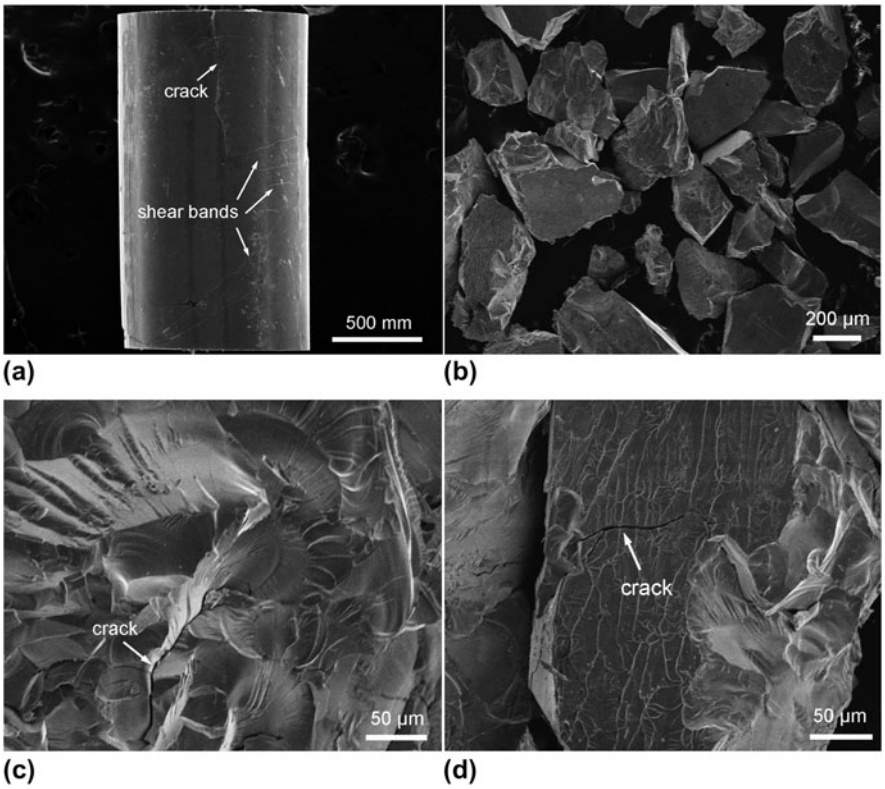


FIG. 4. Scanning electron microscopy images of the deformed and fractured samples for $Co_{60}Ta_5B_{35}$ BMG: (a) the outline surface of the deformed sample; (b) fracture fragments; the morphology of the fragments with (c) shell patterns, and (d) vein-like patterns.

https://doi.org/10.1557/jmr.2011.187 Published online by Cambridge University Press

glasses with low G/B values below 0.41–0.43, or equivalently with high ν above 0.31–0.32 are expected to exhibit significant plastic deformation. In this study, the elastic constants of our Co–Ta–B BMGs with d_c of 2 mm were also measured, as listed in Table II. The values of G/B and ν of the Co-based BMGs are 0.42 and 0.315, respectively, which is within the critical range of G/B and ν for the transition from plastic to brittle fracture behavior. Therefore, we can find both kinds of fracture features for brittle BMGs, (e.g., Mg- and part of Fe Co-based ones) and plastic BMGs (e.g., Zr- and Pd-based ones) in our samples.

C. Correlations among mechanical properties and related properties

As the strongest bulk metallic materials known so far, the ternary Co–Ta–B glassy alloys with simple elemental composition, high thermal stability, ultrahigh hardness, obvious plasticity, and good GFA can be regarded as a good model system to study deformation behavior and mechanism for this kind of ultrahigh strength structural materials. We selected several well-known correlation models regarding mechanical properties and related properties of BMGs, i.e., strength versus elastic modulus, strength versus thermal properties, elastic constants versus thermal properties, and hardness versus elastic modulus, and validated them in our ultrahigh strength Co-based BMG system.

It has been reported that there exists a rough linear relation between compressive strength (σ_c) and Young's modulus (E), i.e., $\sigma_c \approx 0.02E$.[6,7] Considering that the yield strength (σ_y) of metallic glasses is determined by critical shear motion of atomic clusters, Johnson and Samwer[8] built a better linear relationship between shear stress at yielding ($\tau_y = \sigma_y/2$) and shear modulus (G) at room temperature for 30 BMG compositions, as described by:

$$\tau_y = \gamma_c G \quad , \qquad (1)$$

where γ_c is the critical shear strain. Figure 5 shows the relationship between G and τ_y for various BMGs. Our Co-based BMGs obey the linear correlation [Eq. (1)], indicating that the rule is effective in predicting mechanical properties of BMGs with high strength up to 6 GPa. The value of γ_c is revised to be 0.0282 ± 0.0010, which is slightly higher than previously reported value of 0.0267 ± 0.0020.[8]

Early reports implied a possible relationship between strength and thermal properties, i.e., T_g or T_l, in BMG systems.[5,36] By incorporating the molar volume (V), an universal scaling law derived from the fundamental thermodynamics was further proposed by Liu et al.[37] to uncover an inherent relationship of the τ_y with T_g and V. An equation was proposed as:

$$\tau_y = \frac{3R(T_g - T_{RM})}{V} \quad , \qquad (2)$$

where R is the gas constant and T_{RM} is the room temperature. The model has been validated within 15 various BMGs with well-defined yielding in Zr-, Cu-, Ni-, and Fe-based alloy systems. Because of the catastrophic fracture before yielding for all of the reported Co-based BMGs, the validation of this model in Co-based BMGs is not provided. However, the model can be further checked with our plastic Co-based BMGs due to the easy determination of τ_y. Figure 6 shows the values of τ_y as a function of calculated $(T_g - T_{RM})/V$ for 15 various BMGs[37] marked as black circle and our developed Co-based BMGs marked as red square. The slope of the dot line in the τ_y versus $(T_g - T_{RM})/V$ graph is $3R$. The experimental data of our alloys are in good accordance with the calculated ones by Eq. (2). This agreement indicates that mechanical properties for Co-based BMGs can also be predicted using T_g and V.

Moreover, the correlation of T_g (or T_l) with elastic properties was also provided for metallic glasses.[7,9,36,38] Based on the concept of topological fluctuations related through local elastic energy, a universal model, describing a quantitative relationship between T_g and elastic constants, was proposed by Egami et al.,[39] as described by:

TABLE II. Compressive mechanical properties, elastic constants, and related physical properties of $Co_{65-x}Ta_xB_{35}$ (at.%, x = 5–10) BMGs. ρ, V, H_v, σ_y, σ_c, ε_p, E, G, B, and ν are density, molar volume, Vickers hardness, yield strength, compressive strength, plastic strain, respectively. E, G, B, and ν are Young's modulus, shear modulus, bulk modulus, and Poisson's ratio, respectively.

Alloys	ρ (g/cm^3)	V (cm^3/mol)	H_v (GPa)	σ_y (MPa)	σ_c (MPa)	ε_p (%)	E (GPa)	G (GPa)	B (GPa)	G/B	ν	Specific strength (N·m/g)	Specific Young's modulus (kN·m/g)
$Co_{60}Ta_5B_{35}$	8.612	5595	15.0	5190	5630	1.5	–	–	–	–	–	654	–
$Co_{59}Ta_6B_{35}$	8.826	5597	15.2	5410	5720	1.5	–	–	–	–	–	648	–
$Co_{58}Ta_7B_{35}$	8.960	5650	15.4	5420	5800	1.1	240.6	91.5	215.7	0.42	0.315	647	26.8
$Co_{57}Ta_8B_{35}$	9.178	5648	15.5	5515	5875	0.9	240.1	91.3	216.5	0.42	0.315	640	26.2
$Co_{56}Ta_9B_{35}$	9.285	5717	15.9	5590	5970	0.6	246.9	93.8	224.1	0.42	0.315	643	26.6
$Co_{55}Ta_{10}B_{35}$	9.418	5763	16.1	5630	6020	0.5	–	–	–	–	–	639	–

https://doi.org/10.1557/jmr.2011.187 Published online by Cambridge University Press

$$T_g = \frac{2BV(\varepsilon_v^{T,crit})^2}{K_\alpha} \quad , \qquad (3)$$

where $\varepsilon_v^{T,crit}$ is the critical volume strain before the environment relaxes at the temperature T, and $K_\alpha = [3(1–\nu)/2/(1–2\nu)]$ is a factor depending on the Poisson ratio (ν). The value of $\varepsilon_v^{T,crit}$ can be equal to 0.092 at room temperature. The validation of this model was proved in various BMG-forming systems with a wide range of T_g, including the La–Al–Co system with low T_g.[40] Our Co-based BMGs present a high T_g of ~950 K, which is out of the range of the reported evaluation using the model. However, experimental values of T_g and the calculated ones of $2BV/K_\alpha$ exhibit a good match with predicted ones for the Co-based BMGs using the model, which can be identified by the dashed line in Fig. 7. This result indicates that a quantitative relationship between T_g and elastic constants can be extended to Co-based BMGs with high elastic modulus and thermal stability.

The correlation between Young's modulus (E) and Vickers hardness (H_v) as $H_v/E \approx 0.06$ for metallic glasses is proposed by Whang et al.[41] In addition, a more detailed analysis performed by Ohtsuki et al.[30] indicates that the relationship can be built as $H_v/E \approx 0.064 \pm 0.005$ for metal–metal amorphous alloy system and $H_v/E \approx 0.057 \pm 0.007$ for metal–metalloid amorphous system. Recently, the slope of H_v versus E for BMGs was proposed to be ~0.05 by Wang.[7] The discrepancy of the values of H_v/E might be caused by different E values obtained using different testing methods from various reports. In this study, E and H_v obtained via identical testing methods were used for analysis. Ultrasonic pulse-echo evaluation for E and Vickers hardness testing for H_v were used to re-evaluate the relationship between E and H_v for various BMG systems including the Co-based BMGs developed in this study. H_v as a function of E was plotted in Fig. 8. A good linear correlation between E and H_v can be expressed by $H_v/E \approx 0.0615 \pm 0.0070$.

As discussed above, the correlations of compressive mechanical properties with elastic constants and thermal properties for the Co–Ta–B BMGs show good consistency with various well-known universal models so far. The understanding of the deformation mechanism and the design of desirable properties for this kind of ultrahigh strength BMGs are significant in scientific research and industrial applications.

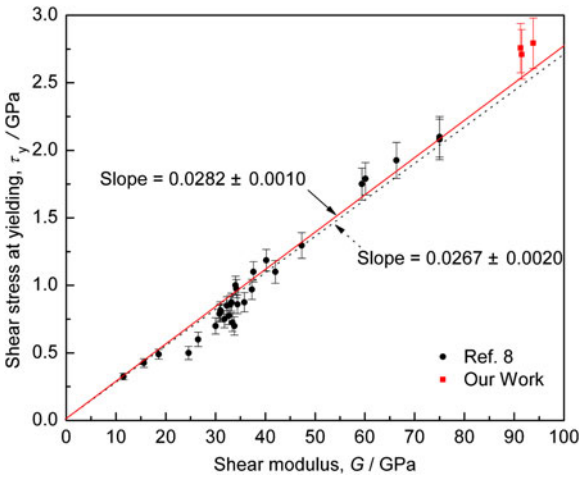


FIG. 5. Relationship between shear stress (τ_y) and shear modulus (G) for various BMGs including the ultrahigh strength Co-based BMGs developed in this study.

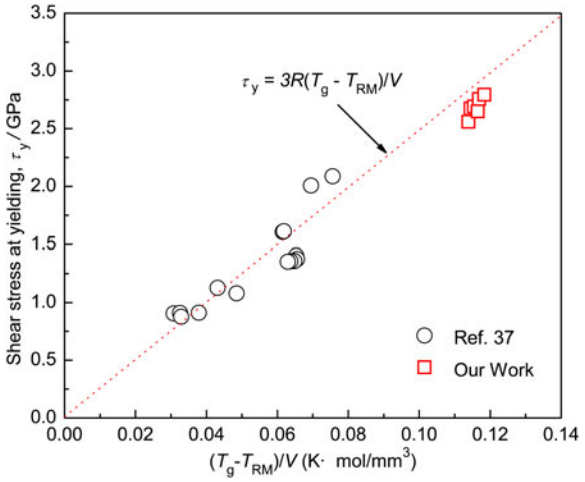


FIG. 6. Relationship between shear stress (τ_y) and $(T_g - T_{RM})/V$ for various BMGs including the ultrahigh strength Co-based BMGs developed in this study. The solid line is plotted following Eq. (2), i.e., $\tau_y = 3R(T_g - T_{RM})/V$.

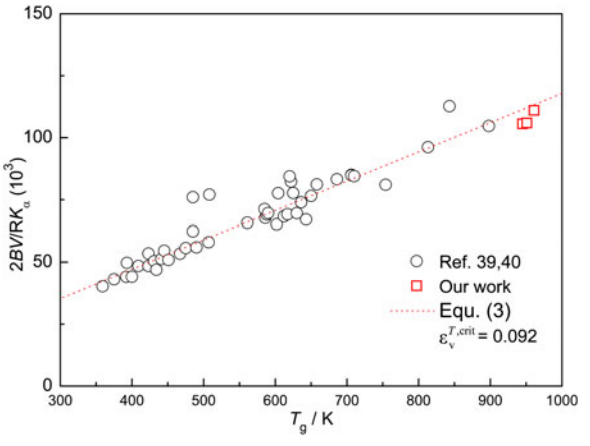


FIG. 7. Correlation between $2BV/RK_\alpha$ and T_g for various BMGs including the ultrahigh strength Co-based BMGs developed in this study. The dashed line is plotted according to Eq. (3) with $\varepsilon_v^{T,crit} = 0.092$.

https://doi.org/10.1557/jmr.2011.187 Published online by Cambridge University Press

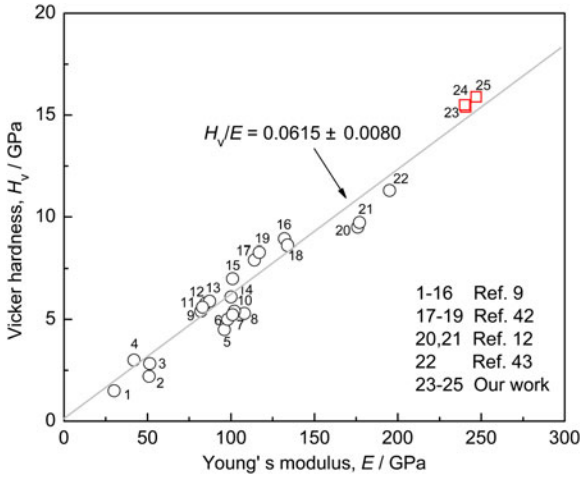


FIG. 8. Relationship between Vickers hardness (H_v) and Young's modulus (E) for various BMGs. The compositions of these BMGs are listed as follows: 1. $Ce_{70}Al_{10}Ni_{10}Cu_{10}$, 2. $Nd_{60}Al_{10}Fe_{20}Co_{10}$, 3. $Mg_{65}Cu_{25}Tb_5$, 4. $La_{55}Al_{25}Cu_{10}Ni_5Co_5$, 5. $Pd_{77.5}Si_{16.5}Cu_6$, 6. $Pd_{40}Ni_{10}Cu_{30}P_{20}$, 7. $Zr_{41}Ti_{14}Cu_{12.5}Ni_{10}Be_{22.5}$, 8. $Pd_{40}Ni_{40}P_{20}$, 9. $Zr_{57}Ti_5Cu_{20}Ni_8Al_{10}$, 10. $Cu_{50}Zr_{45}Al_5$, 11. $Zr_{65}Al_{10}Ni_{10}Cu_{15}$, 12. $Cu_{50}Zr_{50}$, 13. $Zr_{57}Nb_5Cu_{15.4}Ni_{12.6}Al_{10}$, 14. $Zr_{46.75}Ti_{8.25}Cu_{7.5}Ni_{10}Be_{27.5}$, 15. $Cu_{60}Hf_{10}Zr_{20}Ti_{10}$, 16. $Ni_{50}Nb_{50}$, 17. $Ni_{45}Ti_{20}Zr_{25}Al_{10}$, 18. $Ni_{40}Cu_5Ti_{17}Zr_{28}Al_{10}$, 19. $Ni_{39.8}Cu_{5.97}Ti_{15.92}Zr_{27.86}Al_{9.95}Si_{0.5}$, 20. $Fe_{64}Mo_{14}C_{15}B_6Er_1$, 21. $Fe_{64}Cr_3Mo_{10}P_{10}C_{10}B_3$, 22. $Fe_{65}Cr_2Mo_9P_{10}C_8B_6$, 23. $Co_{58}Ta_7B_{35}$, 24. $Co_{57}Ta_8B_{35}$, and 25. $Co_{56}Ta_9B_{35}$.

IV. SUMMARY

The GFA, thermal properties, compressive mechanical properties, and elastic constants of the $Co_{65-x}Ta_xB_{35}$ (at.%, x = 5–10) BMGs produced by copper mold casting were investigated. The following results can be drawn from the above:

(1) The $Co_{65-x}Ta_xB_{35}$ (at.%, x = 5–10) BMGs with critical diameters (d_c) of 1.0–2.0 mm exhibit high glass transition temperature (T_g) of 930 K to 975 K, reduced glass transition temperature (T_{rg}) of 0.61–0.64, supercooled liquid region (ΔT_x) of 41–68 K, and α parameter of 1.17–1.23. The GFA of these alloys is quantitatively correlated with T_{rg} and α.

(2) The alloys show ultrahigh yield strength (σ_y) of 5190–5630 MPa, compressive strength (σ_c) of 5630–6020 MPa, high specific strength of 639–654 N·m/g, and distinct plastic strain (ε_p) of 0.5–1.5% as well as high Vickers hardness of (H_v) up to 16.1 GPa, which are the strongest bulk metallic materials known so far. The fracture morphology shows a mixed feature composed of shell-like and vein-like patterns.

(3) For the Co–Ta–B BMGs developed in this study, the correlations among compressive mechanical strength, elastic moduli, and thermal properties are consistent with various well-known universal criteria of metallic glasses.

ACKNOWLEDGMENTS

This work is supported by the National Basic Research Program (973 Program) (Grant No. 2007CB613900), Natural Science Foundation of China (Grant No. 51071008), and Fundamental Research Funds for the Central Universities.

REFERENCES

1. W.L. Johnson: Bulk glass-forming metallic alloys: Science and technology. *MRS Bull.* **24**, 42 (1999).
2. A. Inoue: Stabilization of metallic supercooled liquid and bulk amorphous alloys. *Acta Mater.* **48**, 279 (2000).
3. M.F. Ashby and A.L. Greer: Metallic glasses as structure materials. *Scr. Mater.* **54**, 321 (2006).
4. W.L. Johnson: Bulk amorphous metal: An emerging engineering material. *JOM* **54**, 40 (2002).
5. A. Ionue, B.L. Shen, and C.T. Chang: Fe- and Co-based bulk glassy alloys with ultrahigh strength of over 4000 MPa. *Intermetallics* **14**, 936 (2006).
6. J.J. Lewandowski and P. Lowhaphandu: Effects of hydrostatic pressure on the flow and fracture of a bulk amorphous metal. *Philos. Mag. A* **82**, 3427 (2002).
7. W.H. Wang: Elastic moduli and behaviors of metallic glasses. *J. Non-Cryst. Solids* **351**, 1481 (2005).
8. W.L. Johnson and K. Samwer: A universal criterion for plastic yielding of metallic glasses with a $(T/T_g)^{2/3}$ temperature dependence. *Phys. Rev. Lett.* **95**, 195501 (2005).
9. W.H. Wang: Correlations between elastic moduli and properties in bulk metallic glasses. *J. Appl. Phys.* **99**, 093506 (2006).
10. Y. Zhang and A.L. Greer: Correlations for predicting plasticity or brittleness of metallic glasses. *J. Alloy. Comp.* **434–435**, 2 (2007).
11. H.W. Sheng, W.K. Luo, F.M. Alamgir, J.M. Bai, and E. Ma: Atomic packing and short-to-medium-range order in metallic glasses. *Nature* **439**, 419 (2006).
12. X.J. Gu, S.J. Poon, G.J. Shiflet, and M. Widom: Ductility improvement of amorphous steels: Roles of shear modulus and electronic structure. *Acta Mater.* **56**, 88 (2008).
13. A. Ionue, B.L. Shen, and C.T. Chang: Super-high strength of over 4000 MPa for Fe-based bulk glassy alloys in $[(Fe_{1-x}Co_x)_{0.75}B_{0.2}Si_{0.05}]_{96}Nb_4$ system. *Acta Mater.* **85**, 4093 (2004).
14. A. Inoue, B.L. Shen, H. Koshiba, H. Kato, and A.R. Yavari: Cobalt-based bulk glassy alloy with ultrahigh strength and soft magnetic properties. *Nat. Mater.* **2**, 661 (2003).
15. A. Inoue: Slowly-cooled bulk amorphous alloys. *Mater. Sci. Forum* **179–181**, 691 (1995).
16. A. Inoue: Bulk amorphous alloys with soft and hard magnetic properties. *Mater. Sci. Eng., A* **226–228**, 691 (1997).
17. http://www.webelements.com.
18. H.A. Davies and B.G. Lewis: Generalized kinetic approach to metallic glass formation. *Scr. Metall.* **9**, 1107 (1975).
19. M.H. Cohen and D. Turnbull: Composition requirements for glass formation in metallic and ionic systems. *Nature* **189**, 131 (1961).
20. W. Klement, R.H. Willens, and P. Duwez: Non-crystalline structure in solidified gold-silicon alloys. *Nature* **187**, 869 (1960).
21. R.J. Highmore and A.L. Greer: Eutectics and the formation of amorphous alloys. *Nature* **339**, 363 (1989).
22. D. Turnbull: Under what conditions can a glass be formed? *Contemp. Phys.* **10**, 473 (1969).
23. A. Inoue, T. Zhang, and T. Masumoto: Glass-forming ability of alloys. *J. Non-Cryst. Solids* **156–158**, 473 (1993).
24. Z.P. Lu and C.T. Liu: A new glass-forming ability criterion for bulk metallic glasses. *Acta Mater.* **50**, 3501 (2002).

https://doi.org/10.1557/jmr.2011.187 Published online by Cambridge University Press

25. S.V. Madge and A.L. Greer: Effect of Ag addition on the glass-forming ability and thermal stability of Mg-Cu-Y alloys. *Mater. Sci. Eng., A* **375–377**, 759 (2004).
26. R. Li, S.J. Pang, C.L. Ma, and T. Zhang: Influence of similar atom substitution on glass formation in (La-Ce)-Al-Co bulk metallic glasses. *Acta Mater.* **55**, 3719 (2007).
27. C.L. Dai, H. Guo, Y. Shen, Y. Li, E. Ma, and J. Xu: A new centimeter-diameter Cu-based bulk metallic glass. *Scr. Mater.* **54**, 1403 (2006).
28. H.X. Li, K.B. Kim, and S. Yi: Enhanced glass-forming ability of Fe-based bulk metallic glasses prepared using hot metal and commercial raw materials through the optimization of Mo content. *Scr. Mater.* **56**, 1035 (2007).
29. M.F. Ashby: *Materials Selection in Mechanical Design*, 3rd ed. (Butterworth-Heinemann, Oxford, UK, 2005), p. 58.
30. M. Ohtsuki, R. Tamura, S. Takeuchi, S. Yoda, and T. Ohmura: Hard metallic glass of tungsten-based alloy. *Appl. Phys. Lett.* **84**, 4911 (2004).
31. A. Inoue, B.L. Shen, A.R. Yavari, and A.L. Greer: Mechanical properties of Fe-based bulk glassy alloys in Fe-Si-B-Nb and Fe-Ga-P-C-B-Si systems. *J. Mater. Res.* **18**, 1487 (2003).
32. M. Stoica, J. Eckert, S. Roth, Z.F. Zhang, L. Schultz, and W.H. Wang: Mechanical behavior of $Fe_{65.5}Cr_4Mo_4Ga_4P_{12}C_5B_{5.5}$ bulk metallic glass. *Intermetallics* **13**, 764 (2005).
33. Z.F. Zhang, H. Zhang, B.L. Shen, A. Inoue, and J. Eckert: Shear fracture and fragmentation mechanisms of bulk metallic glasses. *Philos. Mag. Lett.* **86**, 643 (2006).
34. J.T. Fan, Z.F. Zhang, S.X. Mao, B.L. Shen, and A. Inoue: Deformation and fracture behaviors of Co-based metallic glass land its composite with dendrites. *Intermetallics* **17**, 445 (2009).
35. J.J. Lewandowski, W.H. Wang, and A.L. Greer: Intrinsic plasticity or britttleness of metallic glasses. *Philos. Mag. Lett.* **85**, 77 (2005).
36. A. Ionue and A. Takeuchi: Recent progress in bulk glassy alloys. *Mater. Trans.* **43**, 1892 (2002).
37. Y.H. Liu, C.T. Liu, W.H. Wang, A. Inoue, T. Sakurai, and M.W. Chen: Thermodynamic origins of shear band formation and the universal scaling law of metallic glass strength. *Phys. Rev. Lett.* **103**, 065504 (2009).
38. J.C. Dyre, N.B. Olsen, and T. Chrisrensen: Local elastic expansion model for viscous-flow activation energies of glass-forming molecular liquids. *Phys. Rev. B* **53**, 2171 (1996).
39. T. Egami, S.J. Poon, Z. Zhang, and V. Keppens: Glass transition in metallic glasses: A microscopic model of topological fluctuations in the bonding network. *Phys. Rev. B* **76**, 024203 (2007).
40. R. Li, M. Stoica, G. Wang, and J.M. Park: Glass formation, thermal properties, and elastic constants of La-Al-Co alloys. *J. Mater. Res.* **25**, 1398 (2010).
41. S.H. Whang, D.E. Polk, and B.C. Giessen: The correlation between the Young's modules and microhardness in metallic glasses. *Proceedings of the Fourth International Conference on Rapidly Quenched Metals*, edited by T. Masumoto and K. Suzuki (Japan Institute of Metals, Tokyo, 1982), pp. 1365–1368.
42. D.H. Xu, G. Duan, W.L. Johnson, and C. Garland: Formation and properties of new Ni-based amorphous alloys with critical casting thickness up to 5 mm. *Acta Mater.* **52**, 3493 (2004).
43. X.J. Gu, A.G. McDermott, and S.J. Poon: Critical poisson's ratio for plasticity in Fe-Mo-C-B-Ln bulk amorphous steel. *Appl. Phys. Lett.* **88**, 211905 (2006).

https://doi.org/10.1557/jmr.2011.187 Published online by Cambridge University Press